

Distinct turbulence sources and confinement features in the spherical tokamak plasma regime

This content has been downloaded from IOPscience. Please scroll down to see the full text.

View [the table of contents for this issue](#), or go to the [journal homepage](#) for more

Download details:

IP Address: 198.125.231.54

This content was downloaded on 02/11/2015 at 18:31

Please note that [terms and conditions apply](#).

Letter

Distinct turbulence sources and confinement features in the spherical tokamak plasma regime

W.X. Wang¹, S. Ethier¹, Y. Ren¹, S. Kaye¹, J. Chen¹, E. Startsev¹ and Z. Lu²

¹ Plasma Physics Laboratory, Princeton University, Princeton, NJ 08543, USA

² University of California, San Diego, La Jolla, CA 92093, USA

E-mail: wwang@pppl.gov

Received 20 July 2015, revised 24 September 2015

Accepted for publication 5 October 2015

Published 30 October 2015



CrossMark

Abstract

New turbulence contributions to plasma transport and confinement in the spherical tokamak (ST) regime are identified through nonlinear gyrokinetic simulations. The drift wave Kelvin–Helmholtz (KH) mode characterized by intrinsic mode asymmetry is shown to drive significant ion thermal transport in strongly rotating national spherical torus experiment (NSTX) L-modes. The long wavelength, quasi-coherent dissipative trapped electron mode (TEM) is destabilized in NSTX H-modes despite the presence of strong $\mathbf{E} \times \mathbf{B}$ shear, providing a robust turbulence source dominant over collisionless TEM. Dissipative trapped electron mode (DTEM)-driven transport in the NSTX parametric regime is shown to increase with electron collision frequency, offering one possible source for the confinement scaling observed in experiments. There exists a turbulence-free regime in the collision-induced collisionless trapped electron mode to DTEM transition for ST plasmas. This predicts a natural access to a minimum transport state in the low collisionality regime that future advanced STs may cover.

Keywords: plasma turbulence, transport, confinement, spherical tokamak, drift wave instability

(Some figures may appear in colour only in the online journal)

The low-aspect ratio spherical tokamak (ST) experiments explore an alternative roadmap towards fusion energy production compared to that of conventional tokamaks. STs, such as the national spherical torus experiment (NSTX) and its upgrade NSTX-U, are characterized by high- β (the ratio of plasma pressure to magnetic pressure), very strong toroidal rotation due to neutral beam injected momentum, large ρ^* (the ratio of the ion gyroradius to the plasma minor radius), strong toroidicity and shaping, high fraction of magnetically trapped particles etc. Such highly distinct features result in a different fusion plasma regime with unique physics properties, including transport and confinement behaviors compared to conventional tokamaks.

In general, the free energy associated with non-uniform profiles of magnetically confined non-equilibrium plasmas

drives various micro-instabilities in fusion experiments. The resulting turbulent fluctuations in electric and magnetic fields, density, temperature, and flows are responsible for anomalous particle, momentum and energy transport in such systems. In conventional tokamak regimes, the traditional drift wave instabilities of the ion temperature gradient (ITG) mode and collisionless trapped electron mode (CTEM) are believed to be the prime sources for generating the low-k fluctuations (about and larger than the ion gyroradius scale) and the anomalous transport that are widely observed in experiments. Low-k fluctuations remain important in determining plasma transport and confinement in STs. This is supported by experimental observations that ion toroidal momentum transport is always much higher than the neoclassical level and that ion

energy transport is significantly anomalous in L-modes [1]. It is certainly possible that low-k fluctuations can also drive large energy transport in the electron channel, contributing to the highly anomalous level observed in ST experiments. However, the sources for low-k fluctuations in STs remain unclear. In particular, ST plasmas usually have a very large toroidal rotation that creates a strong $\mathbf{E} \times \mathbf{B}$ flow, and the associated $\mathbf{E} \times \mathbf{B}$ flow shear is often strong enough to stabilize most of the low-k instabilities, including ITG and CTEM. We show that electron collisions can produce an even stronger stabilizing effect on CTEM in the NSTX parametric regime.

The energy confinement time τ_E in NSTX is found to be proportional to the inverse of electron collisionality $\nu_{*,e}$, more specifically $B_T \tau_E \sim \nu_{*,e}^{-0.79}$ [2]. This scaling was observed in NSTX H-modes and will be further tested in the lower collisionality regime of NSTX-U experiments. Understanding the underlying mechanism behind this scaling remains a critical issue [3], which contributes to the important knowledge base needed for developing future advanced ST experiments.

This nonlinear gyrokinetic study focuses on the investigation of distinct turbulence sources responsible for transport and confinement in the unique spherical tokamak regimes. Two nontraditional turbulence sources found to be important in the ST regime through global gyrokinetic simulations of NSTX experiments are the drift wave Kelvin–Helmholtz (KH) instability and the dissipative trapped electron mode (DTEM). For the first time, the KH mode is identified to drive significant transport in realistic fusion experiments. Strong $\mathbf{E} \times \mathbf{B}$ shear is found to have little effect on DTEM identified in NSTX H-modes. DTEM-driven transport in the NSTX parametric regime is shown to produce the same trend as the collisionality scaling of confinement time observed in experiments. The existence of a minimum plasma transport regime that future advanced STs may access is predicted.

The global gyrokinetic simulations carried out with the GTS code [4, 5] for this study include kinetic electrons, taking into account the comprehensive influence of realistic geometry, collisionality, toroidal flow and associated $\mathbf{E} \times \mathbf{B}$ flow.

The toroidal rotation can strongly impact micro-instabilities, particularly long wavelength modes, through its contribution to the equilibrium electric field E_r , for which the associated $\mathbf{E} \times \mathbf{B}$ flow shear can change instability growth rate linearly and cause turbulence decorrelation nonlinearly [6]. Generally, the $\mathbf{E} \times \mathbf{B}$ shear effects on instabilities are strongly mode-dependent, involving the effects on mode structure. The velocity shear, on the other hand, also provides a source of free energy that may drive its own instability and turbulence in magnetized plasmas. This is known as the drift-wave-type Kelvin–Helmholtz (KH) instability [7–11].

The excitation of KH modes in toroidal plasmas requires a large toroidal rotation with a strong gradient to overcome various damping effects, including enhanced Landau damping due to finite k_{\parallel} induced by the intrinsic asymmetry in the KH eigenmode structure, the magnetic shear stabilization, and the $\mathbf{E} \times \mathbf{B}$ shear suppression associated with toroidal rotation gradient. A rough estimate of the threshold for KH excitation is [7, 11]:

$$|ML_n/L\omega_\phi| > 1, \quad (1)$$

where $M = V_\phi/c_s$ is the Mach number with the sound speed $c_s = \sqrt{T_e/m_i}$, $L\omega_\phi$ and L_n are the toroidal rotation and density gradient scale lengths, respectively. For typical tokamak parameters, the threshold for destabilizing KH is hardly achievable [6]. While some numerical simulations of ITG turbulence observed enhanced transport due to high flow shear [12–14], there is no report of observing KH in tokamak experiments, and neither a clear identification of the presence of KH modes from direct numerical simulations for realistic discharges. In the scrape-off layer region of tokamaks, a near-sonic parallel flow with strong shear may arise due to sheath acceleration, and possibly trigger a KH instability as suggested by a previous study [15].

However, the situation can be quite different in ST plasmas. Because of the smaller plasma volume, the momentum input through neutral beam injection (NBI) can drive the ST plasma to rotate much faster than in conventional tokamaks, bringing it into a regime with $M \sim 1$ and a steep rotation gradient where the KH mode could be destabilized. Toroidal flows may also result from intrinsic rotation due to, e.g. fluctuation-generated residual stress. However, compared to the NBI torque, the contribution of intrinsic rotation is small in NSTX. Toroidal rotations in non-NBI-heated NSTX plasmas are always much lower than that of NBI-heated plasmas, and it is unlikely that intrinsic rotation by itself can drive the KH mode unstable in core plasmas. As shown in the left panel of figure 1, a fast rotation ($M \sim 1$) and steep rotation gradient make the KH drive well above the instability threshold in the central core region for an NBI-heated L-mode NSTX discharge [16], suggesting the possible excitation of the mode. Direct linear and nonlinear global gyrokinetic simulations are then carried out for this experiment to provide a clear identification of the KH modes and their role in driving transport.

Unlike most drift wave instabilities in toroidal plasmas, the KH eigenmode structure displays an intrinsic asymmetry. Specifically, the KH modes shift off their rational surface, resulting in a significant finite k_{\parallel} that is proportional to the rotation gradient [8, 11]:

$$k_{\parallel} \sim \frac{k_{\theta} \rho_s}{2c_s} \frac{1}{n} \frac{d(nV_{\parallel})}{dr} \sim \frac{k_{\theta} \rho_s B_\phi}{2c_s B} R \frac{d\omega_\phi}{dr}. \quad (2)$$

This unique feature provides a clear attribute for its identification. Our global simulations cover a radial domain from $r/a = 0.3$ to 0.8. At both the inner and outer radial boundary layers, the gradient drive is set to be zero, and correspondingly, $\nabla\phi = 0$ is used as a boundary condition for the fluctuation potential. Initially, random perturbations at the noise level are given to the distribution functions. The size of the grid cells on the poloidal planes is \sim local ρ_i , and 200 particles/cell per species are used. The equilibrium $\mathbf{E} \times \mathbf{B}$ is set to be zero in our linear simulations. However, for our nonlinear simulations an equilibrium electric field E_r consistently with the initial equilibrium conditions via the radial force balance relation is used. The simulated instability mode structures are illustrated in figure 2. Indeed, in the region where the

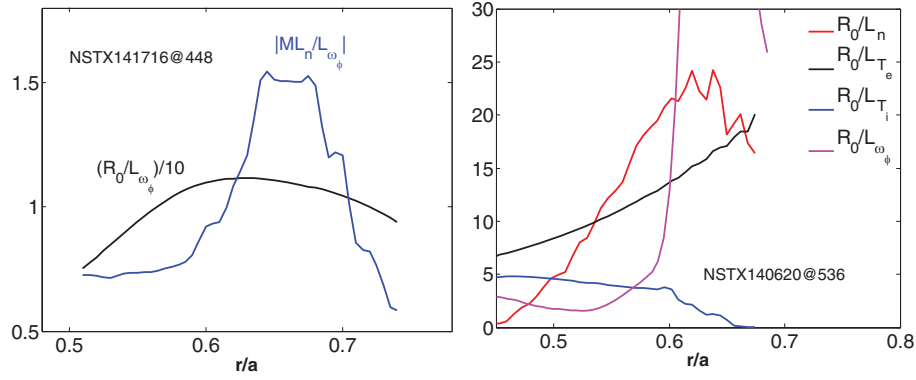


Figure 1. Radial profiles of $|ML_n/L_{\omega_\phi}|$ and toroidal rotation gradient for an NSTX L-mode discharge (left); radial profiles of plasma gradients R_0/L_n , R_0/L_{T_e} , R_0/L_{T_i} and R_0/L_{ω_ϕ} for an NSTX H-mode discharge (right).

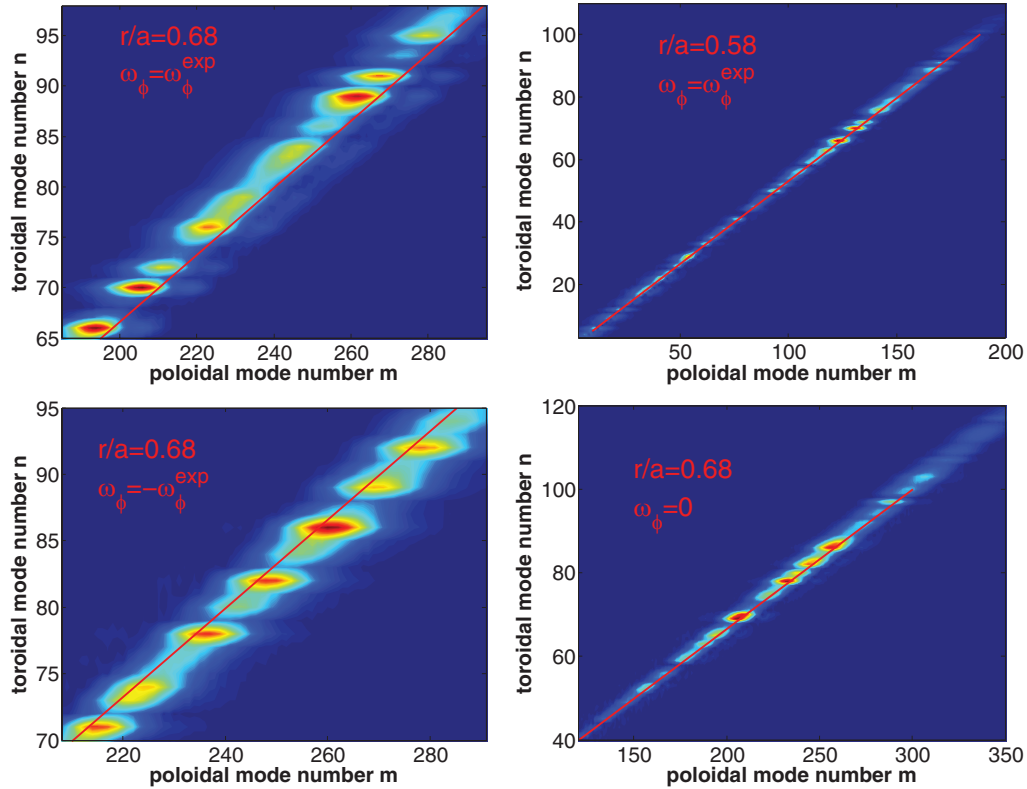


Figure 2. Linear mode spectra $|\delta\Phi_{m,n}|$ at two radial locations (flux surfaces) from simulations using different toroidal rotations: at $r/a = 0.68$ (upper-left) and $r/a = 0.58$ (upper-right) with real toroidal rotation, at $r/a = 0.68$ with inverse rotation (lower-left) and with zero rotation (lower-right). Straight lines indicate mode rational surfaces.

condition of equation (1) is well satisfied, the excited modes are located away from the rational surface to one side (upper-left panel), showing a strong asymmetry. In contrast to this, in the region where the flow shear drive is weak (as indicated in figure 1), unstable modes are basically located on the rational surface (upper-right panel), showing little or weak asymmetry. Note that there is a significant ion temperature gradient in this region, which drives those ITG modes. Moreover, the direction to which the KH modes are shifted away from the rational surface depends on the sign of the rotation gradient.

This can be seen from equation (2). This characteristic is further tested as a fingerprint for the presence of KH modes by a simulation in which we reverse the rotation profile, $\omega_\phi \rightarrow -\omega_\phi$. As shown in the lower-left of figure 2, the unstable modes in this case are shifted away to the other side of the rational surface, consistent with equation (2). Furthermore, when toroidal rotation is zeroed out in the simulation, we only observed ITG modes, which are in a similar range of toroidal mode numbers as that of KH modes, but mostly located on the rational surface (lower-right panel). Therefore, we conclude that the

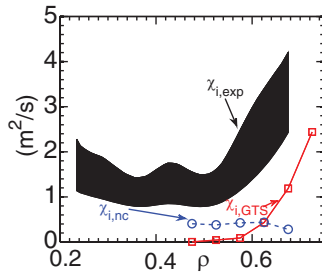


Figure 3. Radial profiles of turbulence-generated and neoclassical ion thermal diffusivities for the L-mode discharge shown in the left panel of figure 1. (Note that GTS simulations only calculate turbulence transport in this study, and neoclassical transport is calculated by GTC-NEO separately.)

drift-wave KH modes are destabilized in NSTX plasmas by strong toroidal rotation produced by NBI. For this specific discharge, both KH and ITG modes co-exist, although the KH modes grow faster than ITGs.

Nonlinearly, the KH instability saturates through energy transfer to longer wavelength, linearly stable modes via toroidal mode coupling, along with strong zonal flow generation, which is a quite robust paradigm observed in most drift wave turbulence systems [17–19]. Furthermore, the equilibrium $\mathbf{E} \times \mathbf{B}$ shear flow associated with the strong rotation gradient is found to have significant influence on low- k fluctuations due to KH and ITG instabilities. Linearly it largely reduces mode growth rate and changes unstable mode family members and structure. Nonlinearly, it modifies the fluctuation amplitude and spectrum. However, the equilibrium $\mathbf{E} \times \mathbf{B}$ shear does not fully suppress the KH/ITG generated turbulence, and finite fluctuations remain, with $e\delta\phi/T_e \sim 1\%$. While it is hard to distinguish KH and ITG fluctuations from each other because they are all in the same low- k range, the KH contribution to the total fluctuations may dominate over ITG as the former's growth rate is larger than the latter's. The remaining low- k fluctuations can produce plasma transport through multiple channels. Particularly, they can produce significant ion thermal transport (larger than the neoclassical one) relevant to the experimental level in the outer core region (figure 3). The sum of the KH/ITG fluctuation driven transport and neoclassical transport, which is calculated from a global GTC-NEO simulation including finite orbit width effect [20], can reproduce the experimental χ_1 profile fairly well (within a factor of two) without significant transport ‘shortfall’ [21, 22] in the outer core region. The simulated toroidal momentum transport due to turbulence is comparable to the experimentally inferred level (about 2–3 times lower). However, KH/ITG driven transport is shown to contribute weakly to the observed, highly anomalous electron thermal transport in NSTX (more than one order of magnitude lower).

The presence of magnetically trapped electrons gives rise to two types of trapped electron modes, CTEM and DTEM, in toroidal plasmas. Each is driven by the free energy provided by the electron density and temperature gradients, but associated with different trapped electron dynamics [23]. CTEM is found to be important in almost all present-day tokamaks, while DTEM is rarely observed in tokamak experiments, and

considered to only play a small role there [24]. We show that in STs DTEM becomes a major source of turbulence, dominant over CTEM, which is opposite to conventional tokamaks.

Our investigation is carried out for an NBI-heated NSTX H-mode discharge [25], where there are strong electron gradients, in particular, the density gradient present in the central core region, along with a very strong toroidal rotation shear and a corresponding strong $\mathbf{E} \times \mathbf{B}$ shear in the region (see the right panel of figure 1). The large gradient in density is due to the temporal proximity to an edge localized mode, but a DTEM is predicted to occur at this density gradient value as well as values that are lower by a factor of three. Unlike the L-mode discharge we studied previously, the KH mode is not excited by the toroidal rotation shear in this case, mainly because of the presence of the strong density gradient, which stabilizes the mode. On the other hand, the strong density gradient is found to drive TEM unstable in the region. Distinguishing DTEM from CTEM is made through mode reactions to electron collisions. Our global simulations cover $\rho/a = 0.3\text{--}0.8$ with focus on $\rho/a \lesssim 0.65$. The linear mode structures represented by potential contour plots in figure 4 clearly show how collisions turn ∇n -driven instability from CTEM to DTEM. When electron collisions are set to be zero (ion collisions are on), the instability excited is CTEM (left panel). The poloidal wavenumber for the most unstable CTEM mode is $k_{\theta\rho_s} \sim 0.5$. As we turn on electron collisions, the unstable modes switch to clearly different ones with much larger structures (middle panel). The most unstable mode now peaks at $k_{\theta\rho_s} \sim 0.1$. Furthermore, it is shown that turning on the ion collisions does not cause the change in mode structure, and only the presence of electron collisions is needed for the longer wavelength modes to be unstable. All these features identify DTEM as the long wavelength modes observed in the simulations of NSTX H-modes with real collision frequencies, which are driven by electron gradients and destabilized by electron collisions.

More interesting linear features of DTEM in comparison with CTEM are presented in the right panel of figure 4. Both DTEM and CTEM have a real frequency close to the ion bounce frequency, $\omega \sim \omega_{b,i}$, falling into the so-called transition regime, which is usually not covered by analytical theory. The most remarkable feature discovered is that the normal $\mathbf{E} \times \mathbf{B}$ shear stabilization effect on DTEM is surprisingly weak (almost negligible), as shown in the right of figure 4. In contrast, the $\mathbf{E} \times \mathbf{B}$ shear can reduce the CTEM growth rate by a factor of ten. Unlike the normal broad-band fluctuations such as ITG and CTEM, the DTEM observed in NSTX shows a large scale, quasi-coherent eddy structure with a few dominant modes, which may make it less affected by the $\mathbf{E} \times \mathbf{B}$ shear. Moreover, unlike the typical ballooning located at the low-field side midplane region, the DTEM appears to also balloon at the region of both top and bottom tips (see figure 4), probably due to the presence of additional magnetic wells there in NSTX. This may make the $\mathbf{E} \times \mathbf{B}$ shearing effect, which has poloidal dependence, weaker. Nevertheless, the strong survivability of DTEM may make it, in the ST regime, a major turbulence source dominant over CTEM. The latter is also subject to strong collisional stabilization in NSTX.

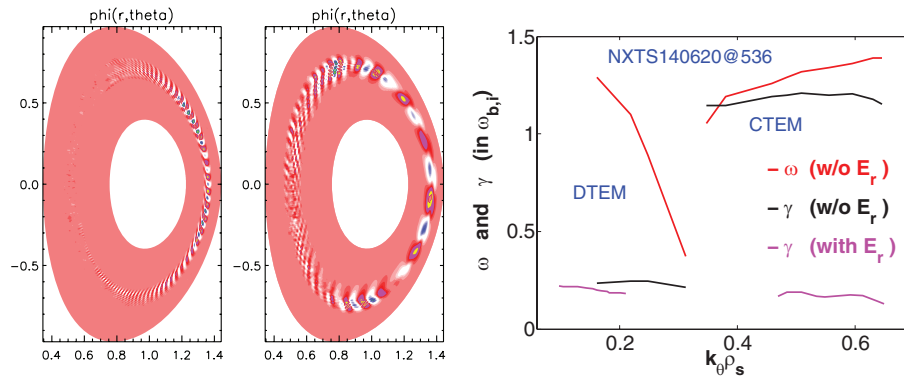


Figure 4. Contour plots of electric potential showing linear mode structures for (left) CTEM ($\nu_i = 1$ and $\nu_e = 0$) and (middle) DTEM ($\nu_i = 1$ and $\nu_e = 1$), and (right) their linear growth rate γ and real frequency ω (normalized by ion bounce frequency $\omega_{b,i}$) versus poloidal wavenumber k_θ from simulations of an NSTX H-mode discharge shown in the right panel of figure 1.

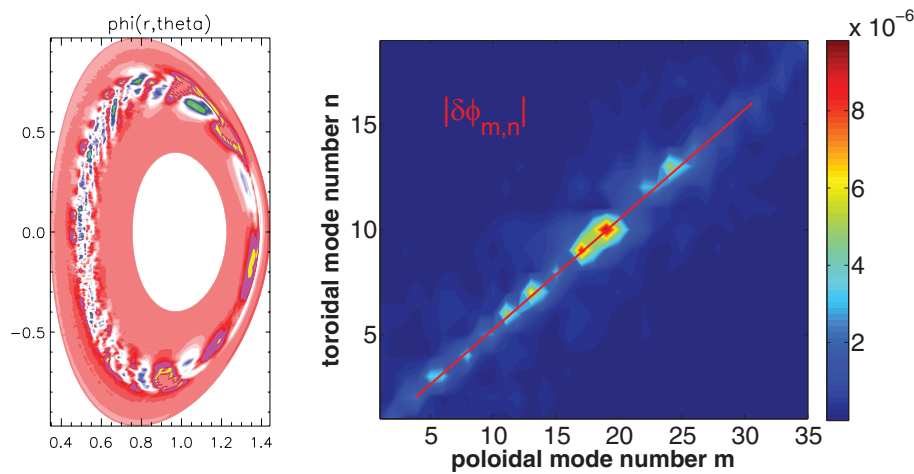


Figure 5. A snapshot of fluctuation potential at saturated DTEM turbulence (left) and spectrum $|\delta\Phi_{mn}|$ (right) from a nonlinear simulation of the NSTX H-mode discharge in figure 1.

The role of DTEM was previously considered in tokamaks [26]. A comparable tokamak case generated using a realistic DIII-D geometry, combined with the same NSTX H-mode plasma gradient profiles as in figure 1, is studied, varying the electron collision frequency from zero to 40 times the real frequency. It is shown that CTEM is persistently present over the wide range of electron collisionality. Increasing the collisionality does not cause a mode switch from CTEM to DTEM, but decreases the CTEM growth rate, and consequently, the CTEM turbulence-driven transport level. This result is consistent with the earlier linear calculations which show that the range of parameters where DTEMs are destabilized by increasing collisionality corresponds to very steep density gradients which can hardly be achieved in present tokamaks [24]. A key geometry factor impacting DTEMs is the inverse aspect ratio $\epsilon = a/R$ which measures the strength of toroidal effects. The strength of DTEM drive depends on the trapped electron fraction ($\sim \epsilon^{1/2}$) which can be close to one in the low aspect ratio STs.

The saturated DTEM turbulence shows a large scale, quasi-coherent eddy structure as seen in a potential contour plot (the left of figure 5). The associated spectrum is narrow and

dominated by a few modes at a low- n range corresponding to $k_\theta \rho_s \sim 0.03$ – 0.08 (the right of figure 5). This characteristic is in contrast to the broad-band fluctuations in typical ITG and CTEM turbulence, and can be utilized to identify DTEM in experiments. The quasi-coherent DTEM fluctuations are found to drive significant plasma transport in multiple channels. As shown in figure 6, DTEM-generated ion energy flux is quite close to the experimental value, and DTEM-induced particle and momentum transport are also close to the experimental level in the central core region where DTEM is unstable. However, the density gradient driven DTEM in this case appears not to produce enough transport to account for the highly anomalous electron energy flux in experiments. It should be noticed that DTEM can also be driven by the free energy provided by the electron temperature gradient in the ST parametric regime. In such cases, our nonlinear simulations show that DTEM-induced electron energy transport can be largely enhanced.

We have shown that DTEM can easily survive an experimental, high level of $\mathbf{E} \times \mathbf{B}$ shear, providing a robust turbulence source for driving transport in the ST regime (note that DTEM could possibly be present in NSTX L-mode plasmas

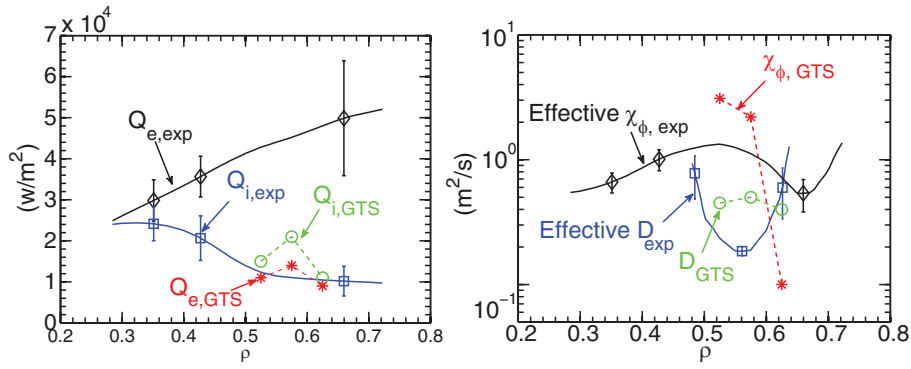


Figure 6. Simulated DTEM driven ion and electron energy fluxes (left), and particle and effective toroidal momentum diffusivity (right) in comparison with experimental values deduced from TRANSP analysis.

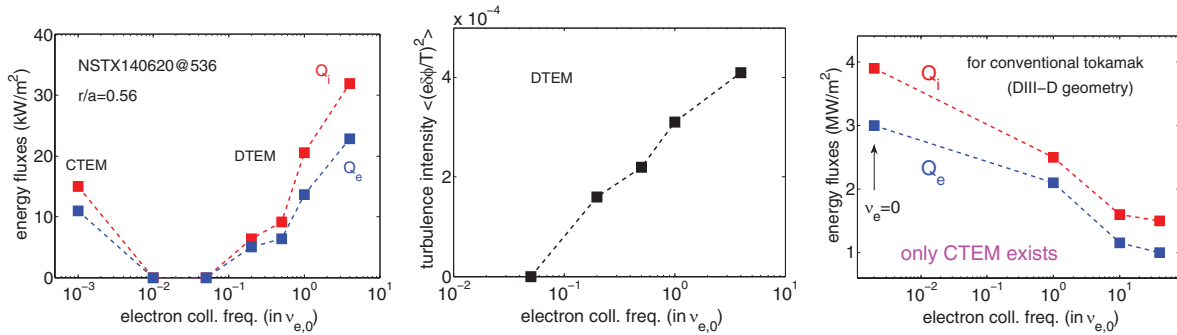


Figure 7. Simulated TEM-driven ion and electron energy flux as a function of electron collision frequency ν_e (normalized by the real frequency) for ST (left) and tokamak (right), and corresponding DTEM turbulence intensity versus ν_e (middle).

as well since a DTEM is predicted to occur at density gradient values much lower than that of the H-mode case reported here.). The role played by collisions in DTEM is subtle and non-trivial [27]. Now we examine how DTEM-driven transport depends on collisions, in particular whether DTEM can contribute to the confinement scaling of ST devices.

A series of nonlinear simulations using the H-mode case of figure 1 are carried out for a collisionality scan, varying the electron collision frequency from zero to four times the real electron frequency. As shown in the left panel of figure 7, change in electron collision frequency causes a turbulence transition from CTEM to DTEM. The collision-induced transition is due to the fact that electron collisions weaken the trapped electron precessional drift resonance with CTEM, and meanwhile, scatter trapped electrons into transit electrons, providing a dissipation mechanism for exciting DTEM. CTEM turbulence is only present in a very low collisionality regime, which is not accessible by NSTX, and even its upgrade NSTX-U. In the NSTX collisionality regime, DTEM-driven transport in all channels, including electron and ion energy flux, is shown to increase close to linearly as the electron collisionality increases. This gives the same trend as the confinement time scaling obtained from the NSTX H-mode database [2]. The increase of transport appears to be associated with the increase in DTEM fluctuation level as collisionality increases (see the middle panel of figure 7). In contrast, CTEM-induced transport in the conventional tokamak regime shows an opposite trend (the right panel of figure 7). This result suggests

that in electron-heated tokamak burning plasmas, such as the ITER regime where electron turbulence is expected to be more important, the plasma confinement may degrade as the heating power increases. One highly interesting result found from this collisionality scan study is that there exists a unique parametric range in collision-induced CTEM to DTEM transition in ST plasmas, in which the collisional drive mechanism, on the one hand, is not strong enough to excite DTEM, and the collisionless drive mechanism (magnetic drift resonance), on the other hand, is also too weak to excite CTEM. If ST experiments are operated in this turbulence-free regime, in principle it may allow access to a minimum transport state and achieve high plasma confinement. Corresponding to this minimum transport state in the CTEM to DTEM transition, the electron collision frequency is about one to two orders of magnitude lower than that of current NSTX plasmas, which may correspond to the collisionality regime of future advanced STs. Beside their direct influence in C/DTEM, collisions may introduce other effects on turbulent transport. For example, change in collision frequency can modify the rate of collisional energy exchange between electrons and ions and consequently the value of T_e/T_i , which is a parameter that can impact the underlying turbulence [28]. However, this occurs in the ion collision time scale which is much longer than that of turbulence, and therefore, its effect is less direct and thus secondary. Collisions may also impact turbulent transport through zonal flow damping [29]. This has more to do with ion collisions rather than electrons. Moreover, the effect of

collisional zonal flow damping on turbulence becomes weaker in the low collisionality regime because time scales for the collisional zonal damping and turbulence development are well separated. Our nonlinear simulations for the collisionality scan include self-consistent zonal flow generation, and the impact of collisional zonal damping on the results is found to be weak.

High- k fluctuations due to electron temperature gradient modes (ETG) may possibly drive significant electron transport in NSTX. It is found that the presence of ETG is very sensitive to the density gradient ∇n in NSTX [30]. For the ∇n -driven DTEM case, such as the H-mode case studied here, ETG can be strongly suppressed by ∇n effects [25]. A minimum transport state with large ∇T_e is also possible if associated ETG can be controlled by finite ∇n . It should be mentioned that microtearing modes (MTM) have been considered as a possible source of turbulence in high- β regime contributing to the NSTX transport, and in particular in the electron channel, and the H-mode confinement scaling [3]. It is also noticed that MTMs could be strongly suppressed by the $\mathbf{E} \times \mathbf{B}$ shear associated with strong toroidal rotation in NSTX. On the other hand, DTEMs appear insensitive to $\mathbf{E} \times \mathbf{B}$ shear. This remains an outstanding issue for further experimental and theoretical studies regarding how these modes can survive and what roles they play under various ST plasma conditions.

Nonlocal transport can be important in fusion plasmas [31]. Our global gyrokinetic simulations in this study take into account some important nonlocal effects, such as turbulence spreading, which may impact global confinement. It should be noted that some nonlocal phenomena, such as transport avalanches associated with flux-driven turbulence, are not considered in our gradient-driven turbulence simulations. There is experimental evidence that nonlocal transport, possibly related to flux-driven turbulence, was present in RF-heated NSTX plasmas [32]. The prediction of the minimum transport state is made without taking flux-driven turbulence into account. Finally, we point out that our current nonlinear gyrokinetic studies focus on electrostatic turbulence regime. It would be highly interesting to investigate how KH and DTEM turbulence and transport are modified by electromagnetic effects due to high- β values in ST

plasmas. This is a largely unexplored topic, which should be addressed in the future.

Acknowledgments

Useful discussions with Drs T.S. Hahm, G. Rewoldt, X. Tang, W.W. Lee and G. Hammett are acknowledged. Simulations were performed on Edison at NERSC. This work was supported by US DOE Contract No. DE-AC02-09CH11466.

References

- [1] Kaye S.M. *et al* 2009 *Nucl. Fusion* **49** 045010
- [2] Kaye S.M. *et al* 2013 *Nucl. Fusion* **53** 063005
- [3] Guttenfelder W. *et al* 2013 *Nucl. Fusion* **53** 093022
- [4] Wang W.X. *et al* 2006 *Phys. Plasmas* **13** 092505
- [5] Wang W.X. *et al* 2010 *Phys. Plasmas* **17** 072511
- [6] Terry P.W. 2000 *Rev. Mod. Phys.* **72** 109
- [7] Catto P.J. *et al* 1973 *Phys. Fluids* **16** 1719
- [8] Drake J.F. *et al* 1992 *Nucl. Fusion* **32** 1657
- [9] Artun M. and Tang W.M. 1992 *Phys. Fluids B* **4** 1102
- [10] Dong J.Q. and Horton W. 1993 *Phys. Fluids B* **5** 1581
- [11] Garbet X. *et al* 1999 *Phys. Plasmas* **6** 3955
- [12] Dimits A.M. *et al* 2001 *Nucl. Fusion* **40** 1725
- [13] Barnes M. *et al* 2011 *Phys. Rev. Lett.* **106** 175004
- [14] Highcock E.G. *et al* 2012 *Phys. Rev. Lett.* **109** 265001
- [15] Schwander F. *et al* 2011 *J. Nucl. Mater.* **415** S601
- [16] Ren Y. *et al* 2013 *Nucl. Fusion* **53** 083007
- [17] Chen L. *et al* 2005 *Phys. Control. Fusion* **47** B71
- [18] Lin Z. *et al* 2005 *Phys. Plasmas* **12** 056125
- [19] Wang W.X. *et al* 2007 *Phys. Plasmas* **14** 072306
- [20] Wang W.X. *et al* 2006 *Phys. Plasmas* **13** 082501
- [21] Holland C. *et al* 2009 *Phys. Plasmas* **16** 052301
- [22] Rhodes T. *et al* 2011 *Nucl. Fusion* **51** 063022
- [23] Kadomtsev B.B. and Pogutse O.P. 1971 *Nucl. Fusion* **11** 67
- [24] Romanelli M. *et al* 2007 *Phys. Plasmas* **14** 082305
- [25] Ren Y. *et al* 2011 *Phys. Rev. Lett.* **106** 165005
- [26] Similon P.L. and Diamond P.H. 1984 *Phys. Fluids* **27** 916
- [27] Connor J.W. *et al* 2006 *Plasma Phys. Control. Fusion* **48** 885
- [28] Doyle E.J. *et al* 2007 *Nucl. Fusion* **47** S18
- [29] Lin Z. *et al* 1999 *Phys. Rev. Lett.* **83** 3645
- [30] Ren Y. *et al* 2012 *Phys. Plasmas* **19** 056125
- [31] Iida K. *et al* 2015 *Nucl. Fusion* **55** 013022
- [32] Ren Y. *et al* Fast response of electron-scale turbulence to auxiliary heating cessation in National Spherical Torus Experiment *Phys. Plasmas* submitted